### Title
Water and heat transport in boreal soils: implications for soil response to climate change.




### Journal
The Science of the total environment, 409(10)

### ISSN
0048-9697



### Authors
Fan, Zhaosheng
Neff, Jason C
Harden, Jennifer W
et al.



### Publication Date
2011-04-01

### DOI
10.1016/j.scitotenv.2011.02.009

Science of the Total Environment 409 (2011) 1836–1842

Contents lists available at ScienceDirect

Science of the Total Environment

journal homepage: www.elsevier.com/locate/scitotenv

# Water and heat transport in boreal soils: Implications for soil response to climate change

Zhaosheng Fan [a,*], Jason C. Neff [a], Jennifer W. Harden [b], Tingjun Zhang [c], Hugo Veldhuis [d], Claudia I. Czimczik [e], Gregory C. Winston [e], Jonathan A. O'Donnell [f]

[a] Department of Geological Sciences, University of Colorado, Boulder, CO 80305, USA
[b] U.S. Geological Survey, Menlo Park, CA 94025, USA
[c] National Snow and Ice Data Center, Cooperative Institute for Research in Environmental Sciences, University of Colorado, Boulder, CO 80305, USA
[d] Agriculture and Agri-Food Canada, University of Manitoba, Winnipeg, MB, Canada R3T 2N2
[e] Department of Earth System Science, University of California, Irvine, CA 92697, USA
[f] Department of Biology and Wildlife, University of Alaska, Fairbanks, AK 99775, USA

ARTICLE INFO

*Article history:*
Received 26 October 2010
Received in revised form 3 February 2011
Accepted 7 February 2011
Available online 26 February 2011

*Keywords:*
Boreal
Carbon
Climate change
Water movement
Water vapor
Permafrost

ABSTRACT

Soil water content strongly affects permafrost dynamics by changing the soil thermal properties. However, the movement of liquid water, which plays an important role in the heat transport of temperate soils, has been under-represented in boreal studies. Two different heat transport models with and without convective heat transport were compared to measurements of soil temperatures in four boreal sites with different stand ages and drainage classes. Overall, soil temperatures during the growing season tended to be over-estimated by 2–4 °C when movement of liquid water and water vapor was not represented in the model. The role of heat transport in water has broad implications for site responses to warming and suggests reduced vulnerability of permafrost to thaw at drier sites. This result is consistent with field observations of faster thaw in response to warming in wet sites compared to drier sites over the past 30 years in Canadian boreal forests. These results highlight that representation of water flow in heat transport models is important to simulate future soil thermal or permafrost dynamics under a changing climate.



## 1. Introduction

A large fraction (approximately 33–37%) of terrestrial carbon (C) is stored in boreal soils (Ping et al., 2008; Tarnocai et al., 2009b). Over the last four decades, air temperatures in the boreal region have increased during winter and spring by 0.2 to 0.3 °C per decade, accompanied by increased precipitation in autumn and winter (Jones and Moberg, 2003; Smith and Reynolds, 2005). In some regions, higher air temperatures are likely triggering increases in net primary production (Bond-Lamberty et al., 2004) as well as changes in soil hydrology (Striegl et al., 2007; Walvoord and Striegl, 2007).

Changes in boreal hydrology may result in a positive feedback to global warming, either via increased emissions of $CH_4$ in previously frozen and now flooded areas or via increased production of $CO_2$ from decomposition or combustion in drained areas. Hydrological changes might also shift the distribution of peatlands, wetlands, and lakes (Rapalee et al., 1998; Vitt et al., 2000). While in some areas thawing of permafrost can promote the development of wetlands and lakes (thermokarst), in other areas permafrost degradation can lead to drainage (Jorgenson and Osterkamp, 2005). In central Siberia, 11% of lakes >40 ha have shrunk or disappeared between 1973 and 1997/1998 (~93,000 ha of regional lake surface) (Smith et al., 2005). Degradation of permafrost over the last two decades has been reported from northern Alaska (Jorgenson et al., 2001), yet the environmental factors responsible for the loss of permafrost are debated with evidence for both the direct effects of warmer temperatures and/or the effects of increasing precipitation (Agafonov et al., 2004).

Heat transport through soils is a critical factor in determining how permafrost changes in response to climate. In most of the existing biophysical models used in boreal settings, pure heat conduction, which is mainly influenced by the particle contact area (Jury and Horton, 2004), is assumed to be the main mechanism of heat transport in the soils. However, heat conduction is not the only mechanism for heat transport in soils and ecosystems. Cahill and Parlange (1998) indicated that liquid water and thermally-induced vapor movement (convection) contributed to ~50% of soil heat flux in temperate soils. In boreal soils where moisture is highly variable across space and through seasons, the role of water movement could be an important factor in seasonal soil energy dynamics and in the long term response of boreal systems to changes in climate. Additionally, the convection of latent heat by water vapor movement

* Corresponding author. Tel.: +1 303 735 2413; fax: +1 303 492 2606.
*E-mail address:* fanz@colorado.edu (Z. Fan).

0048-9697/$ – see front matter © 2011 Elsevier B.V. All rights reserved.
doi:10.1016/j.scitotenv.2011.02.009

in response to temperature gradients will release energy through evaporation–condensation processes, resulting in rapid heat transfer with only minor changes in soil moisture content (Jury and Horton, 2004; Kane et al., 2001).

Two heat transport models used to describe soil thermal dynamics were compared in this study. In Model 1, heat was transported by conduction and convection via the movement of liquid water and water vapor; in Model 2 heat was transported exclusively by conduction, a formulation similar to the commonly used soil physical models for boreal soils, for example, FORFLUX (Zeller and Nikolov, 2000), CLASS (Verseghy, 1991), LPJ-GUESS (Wolf et al., 2008), and Wetland-DNDC (Zhang et al., 2002).

## 2. Material and Methods

We studied three black spruce stands (*Picea mariana* (MILL.) BSP) on well drained, effectively dry ('D') sites that burned in stand-replacing fires in approximately 1964, 1930 or 1921 (Table 1). The well drained sites tend to have gravel subsurface substrates that are highly permeable and tend to inhibit the retention of water and formation of ice-rich permafrost. The well drained 1964 and 1930 sites (1964D and 1930D) were established in years 2003 and 2002 near Thompson, Manitoba, Canada, while the well drained 1921 site (1921D) was established in year 2000 and is located within the Donnelly Flats near Delta Junction, Alaska. We also examined one black spruce stand on a poorly drained, wet ('W') soil that burned in approximately 1964 (1964W) which is located in Manitoba, Canada (Table 1) (Litvak et al., 2003; Manies et al., 2003).

### 2.1. Field Experiments

Field experiments to measure soil temperature and moisture in the organic layers and mineral soil for 1964D, 1930D, and 1964W are presented in the following sections, while Fan et al. (2008) and Manies et al. (2003) contain field experimental details for 1921D. The amounts of organic carbon (OC) present in the mineral soils were similar at all sites and approximately $0.02 \pm 0.01$ g C $cm^{-3}$.

**Table 1**
Descriptions of the four black spruce forest sites[a,b].

| Site name | Site descriptions | Mass of organic layer (g $cm^{-2}$) |
|---|---|---|
| 1964D | 0–1 cm: live *Rhytidium* sp.<br>1–7 cm: fibric C with char<br>Below 7 cm: mineral soil | 0.18 |
| 1930D | 0–3 cm: live *Pleurozium* sp.<br>3–6 cm: dead moss with litter<br>6–11 cm: fungi, roots, and dead moss<br>11–15 cm: lightly to moderately decomposed roots, moss, and wood<br>15–17 cm: charred and decomposed organic matter<br>Below 17 cm: mineral soil | 0.39 |
| 1921D | 0–2 cm: live moss, lichen, and litter<br>2–4 cm: dead moss and litter<br>4–5 cm: lightly decomposed organic matter and roots<br>5–11 cm: moderately decomposed organic matter<br>Below 11 cm: mineral soil | 0.29 |
| 1964W | 0–1 cm: live *Sphagnum* sp.<br>1–10 cm: dead moss with litter and roots<br>10–20 cm: lightly decomposed roots and moss<br>20–25 cm: moderately decomposed organic matter<br>25–35 cm: black and brown amorphous organic matter<br>35–40 cm: black amorphous organic matter<br>Below 40 cm: mineral soil | 0.63 |

[a] Manies et al. (2006, 2003).
[b] The soil horizons were classified based on the method described in Harden et al. (2006).

#### 2.1.1. Field Installations

At 1930D site, one soil pit, excavated by shovel to depth of the C horizon (102–136 cm), was instrumented and backfilled in September 2002, and measured continuously until 2005. At 1964D and 1964W sites, one similar soil pit was instrumented in May 2003 and measured until September 2004.

Precision interchangeable thermistors (model EC95H303W Thermometrics, Edison, NJ, USA) encapsulated in thermally conductive epoxy were inserted horizontally at 2, 6, 14, 30, 50, 70, and 80 cm for 1964D, at 15, 25, 30, 35, 45, and 60 cm for 1964W, and at 6, 11, 16, 18, 29, 41, and 55 cm for 1930D. Time domain reflectrometry soil moisture probes (model CS616, Campbell Scientific Inc., Logan, UT, USA) were also inserted horizontally at 5, 14, 30, 50, and 70 cm for 1964D, at 5, 25, 35, 45, and 60 cm for 1964W, and at 18, 29, 41, and 55 cm for 1930D. Temperature and moisture conditions at the soil surface were monitored with an additional thermistor and a fuel moisture sensor ('fuel rod') (model CS505, Campbell Scientific Inc.).

For monitoring moisture content of near-surface organic soils, 20 cm long ECH2O dielectric constant probes (Decagon Devices, Inc., Pullman, WA, USA) were placed 5 cm below the moss surface at the 1964D and 1964W sites. ECH2O probes have a reported accuracy of 3% and resolution of 0.1%, but we found larger errors (10 to 30% moisture content) when these instruments were calibrated in the lab with soil blocks from each site. These blocks were saturated and then allowed to air-dry while moisture content (by volume) and probe output were monitored. Probe output was plotted against volumetric water content and a linear fit was determined for each site. Factory calibrations were used for TDR and thermistors.

All thermistor, TDR, and ECH2O data were collected and recorded using a data logger (model CR10X, Campbell Scientific Inc.).

#### 2.1.2. Soil Sampling

Detailed methods can be found in Manies et al. (2006). At each site, soil pits were also excavated by shovel to depth of the C horizon (102–136 cm) in years 2001 to 2004. In addition, small pits were excavated for describing organic soil layers, generally to depths of 20 to 50 cm. These excavations were placed 20 m apart along transects about 200 m long. Soils were described according to USDA-NRCS (Soil Survey Division Staff, 1998) and Canadian (Committee CASC, 1998) methodologies and sampled by soil horizons. Samples were analyzed for bulk density and C content. In addition, volumetric soil moisture content was measured using a variety of tools, including a Soil Moisture Equipment Corporation (Goleta, CA) Model 0200 core for deep mineral soils; rectangles of known area (for litter and organic horizons); and cores of various diameters.

#### 2.1.3. Laboratory Analyses

All soil samples were immediately placed on open shelves in an isolated room after shipped to U.S.G.S, and allowed to air dry to a constant weight. Temperature during air-drying ranged from 20 to 30 °C and relative humidity during air-drying ranged from 50 to 60%. Once air dried, samples were separated into archive and moisture/analytical splits. Air dry moisture content of both splits was recorded. Bulk density calculations assumed that the air-to-oven dry moisture ratio in the entire sample was the same as for the moisture/analytical split.

### 2.2. Model Description

The following partial differential equation describes the heat transport by conduction with phase change, plus by the movement of

liquid water and water vapor (Cahill and Parlange, 1998; Hansson et al., 2004; Jones and Moberg, 2003; Lundin, 1985; Saito et al., 2006):

$$C_p\frac{\partial T}{\partial t}+L_0\frac{\partial \theta_v}{\partial t}-L_f\rho_i\frac{\partial \theta_i}{\partial t}=K_t\frac{\partial^2 T}{\partial z^2}-C_w\frac{\partial q_L T}{\partial z}-L_0\frac{\partial q_v}{\partial z}-C_v\frac{\partial q_v T}{\partial z} \quad (1)$$

where $C_p$, $C_w$, and $C_v$ are volumetric heat capacities ($J\,cm^{-3}K^{-1}$) of soil matrix, liquid water, and water vapor, respectively; $T$ is the soil temperature (K); $t$ is the time (day); $L_0$ is the volumetric latent heat of vaporization of liquid water ($J\,cm^{-3}$); $\theta_v$ is the volumetric fraction ($cm^3\,cm^{-3}$) of water vapor; $L_f$ is the latent heat of freezing ($J\,cm^{-3}$); $\rho_i$ is the density of ice ($g\,cm^{-3}$); $\theta_i$ is the volumetric fraction of ice ($cm^3\,cm^{-3}$); $K_t$ is the thermal conductivity ($J\,cm^{-1}\,day^{-1}K^{-1}$) of soil matrix; $z$ is the soil depth (cm); $q_L$ and $q_v$ are the velocity ($cm\,day^{-1}$) of liquid water and water vapor. $C_p$ and $K_t$ are defined as (Weiss et al., 2006):

$$C_p=\begin{cases}C_s\theta_s+C_w\theta_w+C_{OC}\theta_{OC}+C_i\theta_i & \text{for mineral soil}\\ C_w\theta_w+C_{OC}\theta_{OC}+C_i\theta_i & \text{for organic layer}\end{cases} \quad (2)$$

$$K_t=\begin{cases}K_s\theta_s+K_w\theta_w+K_{OC}\theta_{OC}+K_i\theta_i & \text{for mineral soil}\\ K_w\theta_w+K_{OC}\theta_{OC}+K_i\theta_i & \text{for organic layer}\end{cases} \quad (3)$$

where $C_s$, $C_{OC}$, and $C_i$ are volumetric heat capacities ($J\,cm^{-3}K^{-1}$) of mineral soil, organic carbon (OC), and ice, respectively; $\theta_s$, $\theta_w$, and $\theta_{OC}$ are the volumetric fraction ($cm^3\,cm^{-3}$) of mineral soil, liquid water, and OC, respectively; $K_s$, $K_w$, $K_v$, $K_{oc}$, and $K_i$ are the thermal conductivities ($J\,cm^{-1}\,day^{-1}K^{-1}$) of mineral soil, liquid water, water vapor, OC, and ice, respectively. Due to the significantly low volumetric fraction of water vapor and the significantly low volumetric heat capacity of air, water vapor and air were assumed to have negligible impacts on the heat capacity and thermal conductivity of the soil matrix. Also, it was assumed in the model that the fraction of mineral soil particles in the organic layers was negligible. The thermal conductivity of dry mineral soil was related to the soil texture and structure, and defined as a function of bulk density (Lu et al., 2007):

$$K_s=-0.56\left(1-\frac{BD}{PD}\right)+0.51 \quad (4)$$

where $BD$ is the bulk density of mineral soil ($g\,cm^{-3}$); $PD$ is the particle density of mineral soil that is assumed to be $2.65\,g\,cm^{-3}$.

The flux densities of liquid water ($q_L$) and water vapor ($q_v$) are defined as (Cahill and Parlange, 1998; Saito et al., 2006):

$$q_L=-\lambda_{sat}S_e^{0.5}\left[1-\left(1-S_e^{1/m}\right)^m\right]^2\left(\frac{\partial h}{\partial z}+1\right)\ \text{with}\ S_e=\frac{\theta_w-\theta_r}{\theta_{sat}-\theta_r}\ \text{and}\ m=1-\frac{1}{n} \quad (5)$$

$$q_v=-\frac{\tau\theta_a D_a e^{\frac{hMg}{RT}}}{\rho_w}\frac{d\rho_{sv}}{dT} \quad (6)$$

where $\lambda_{sat}$ is the saturated hydraulic conductivity ($cm\,day^{-1}$); $S_e$ is the effective saturation (unitless); $m$ or $n$ is the empirical parameter that constrains the shape of water retention curve (unitless); $h$ is the pressure head (cm); $\theta_{sat}$ and $\theta_r$ are the saturated and residual moisture content ($cm^3\,cm^{-3}$), respectively; $\tau$ is the tortuosity (unitless); $D_a$ is the diffusivity of water vapor in air ($cm^2\,day^{-1}$); $M$ is the molecular weight of water ($g\,mol^{-1}$); $g$ is the gravitational acceleration ($cm\,day^{-1}$); $R$ is the universal gas constant; $\rho_{sv}$ is saturated vapor density ($g\,cm^{-3}$); $\rho_w$ is the density of water ($g\,cm^{-3}$). The tortuosity ($\tau$), diffusivity of water vapor ($D_a$), and saturated vapor density ($\rho_{sv}$) are defined as (Saito et al., 2006):

$$\tau=\frac{\theta_a^{7/3}}{\theta_s^2} \quad (7)$$

$$\rho_{sv}=10^{-3}\times\frac{e^{37.3716-7.92495\times10^{-3}T-\frac{6014.79}{T}}}{T} \quad (8)$$

$$D_a=2.12\times10^{-5}\left(\frac{T}{273.15}\right)^2. \quad (9)$$

One of the difficulties of simulating water flow is unstable flow regimes (e.g., fingering and preferential flow) during water redistribution due to the soil heterogeneity, especially within the organic layers where water flows quickly through the macropores. The water flow in our model was assumed to follow kinematic wave approximation (water flows downward under one unit pressure gradient) for surface organic layers (i.e., live moss, dead moss, lightly and moderately decomposed organic matter, and humic OC of dry sites) due to the large proportion of macropores and lack of wicking of water by feather moss (Wang et al., 2003). Kinematic wave approximation has been successfully used to describe the one-dimensional vertical unsaturated subsurface flow (Germann, 1985), snowmelt water movement (Singh et al., 1997), soil moisture dynamics (Mdaghri-Alaoui and Germann, 1998), and preferential flow (Simunek et al., 2003) in coarse soil with high saturated hydraulic conductivity. The water flows upward or downward in the humic OC (i.e., well decomposed organic matter) of wet sites (Devito et al., 1998; Reeve et al., 2000; Romanowicz et al., 1993) due to the wicking of water by *sphagnum* moss (Wang et al., 2003) and in the mineral soil layers, based on the gradient of soil water pressure head that was defined as:

$$h=\begin{cases}0 & \text{for}\ \theta_w=\theta_s\\ -\left(S_e^{-\frac{1}{m}}-1.0\right)^{1/n}/\alpha & \text{for}\ \theta_w<\theta_s\end{cases} \quad (10)$$

where $\alpha$ is an empirical parameter.

It is extremely difficult to accurately simulate the soil moisture content in the boreal region due to the complicated OC settings, overland runoff, precipitation (including rainfall intensity and duration), evapotranspiration, root water uptake, and latent water flow. Therefore, we did not simulate the soil water content in this study. Instead, we used the daily average values of measured soil moisture content to calculate the daily average values of soil water pressure heads (using Eq. (10)), which can then be used to calculate the daily average values of water flow.

Eq. (1) does not include the impacts of heat of wetting on soil thermal dynamics. Heat of wetting is the heat released during infiltration when very dry soil (e.g., oven-dried) is "completely immersed" by soil water (Prunty and Bell, 2005). Heat of wetting is strongly related to soil water and clay content (Prunty and Bell, 2005). Higher clay content and lower water content tend to lead to release more heat of wetting during water infiltration and this factor is important for heat transport in some soils. However, it is reasonable to assume that heat of wetting has minor impacts on the soil thermal dynamics in our study due to the two following reasons. First, heat of wetting is likely negligible for the deep soil (>6 cm) due to the high initial water content during infiltration/precipitation (>0.2 $cm^{-3}\,cm^3$ compared to 0.00–0.05 $cm^3\,cm^{-3}$ initial soil water content used in Prunty and Bell's, 2005 studies). Second, although the surface soil might release some amount of heat of wetting during water infiltration due to the dry soil condition, infiltration/precipitation events into dry surface soils occur only a handful of times during the

period of our simulations and would have a negligible effect on the overall heat flux to depth examined in this study.

The thermal conductivity of dry OC for each organic layer (i.e., live moss, dead moss and lightly decomposed, moderately decomposed, and well decomposed organic matter) was parameterized based on the laboratory results of O'Donnell et al. (2009) and assigned to different sites based on the distribution of each organic layer (see supplementary material for more details).

The saturated hydraulic conductivity ($\lambda_{sat}$) of the organic layers is also strongly related to the structure and components of organic matter. The surface moss layer has significantly high $\lambda_{sat}$ in comparison to the deep organic matter (such as mesic and humic). The saturated hydraulic conductivity and parameters (i.e., $\alpha$, $n$, $\theta_{sat}$, and $\theta_r$) for van Genuchten water retention curve (Eq. (10)) were set separately for individual organic layers (Price et al., 2008) (see supplementary material for more details). The saturated hydraulic conductivity ($\lambda_{sat}$), $\alpha$, $m$, $\theta_{sat}$, and $\theta_r$, for the mineral soil were estimated using ROSETTA based on the soil texture (Schaap et al., 2001). For the well drained site, the mineral soil was approximately comprised of 43.8% sand, 47.4% silt, and 8.9% clay. For the poorly drained site, the mineral soil was classified as clay according to the USDA soil texture classification (Soil Survey Division Staff, 1993). Therefore, the soil texture was assumed to be clay (clay content>55%) for the poorly drained site. The mineral soil was assumed to be homogeneous and physical properties maintained constant throughout the mineral soil profile.

Eq. (1) can be reduced to the traditional heat transport with only conduction of sensible heat by setting $\theta_v = 0$, $q_w = 0$, and $q_v = 0$,

$$C_p \frac{\partial T}{\partial t} - L_f \rho_i \frac{\partial \theta_i}{\partial t} = K_t \frac{\partial^2 T}{\partial t^2}. \quad (11)$$

The upper and lower boundary conditions were set to the measured (or interpolated) daily average soil temperatures at 0 cm and 50 cm. The soil moisture profile was generated through linear interpolation.

The thermal properties of frozen soil (e.g., soil thermal conductivity and heat capacity) were treated in the same manner as the unfrozen soil and were calculated from Eqs. (2) and (3) based on the ice content, liquid water content, OC and mineral soil fractions. The hydraulic properties of frozen soil (e.g., unsaturated soil hydraulic conductivity) were treated in the same manner as the dry unfrozen soil. In other words, the freezing has the same impacts as drying in that the soil matric potential is reduced thus driving the water flow upward or downward toward the freezing fronts (Hansson et al., 2004).

Eqs. (1) and (11) were solved using a finite difference solver, CVODE (Soil Survey Division Staff, 1993) which is suitable for stiff and non-stiff problems, with the backward differentiation formula integration method and Newton iteration. Both absolute and relative error tolerances were set to 0.001 as the simulation progresses. The soil column was discretized equally into 100 soil layers, resulting in a layer thickness of 0.5 cm during the simulations. The time step size varied between the predefined minimum and maximum time steps of 0 and 1 day, respectively, until the calculation error was within the absolute and relative error tolerances.

The soil temperatures for the three dry sites were simulated for a one-year period, while for the wet site (i.e., 1964W) from 02/2004 to 09/2004. This is due to the incomplete and/or discontinuous observations on soil temperature and moisture during other time periods (e.g., for more than six months).

## 3. Results and Discussion

The comparisons of the calculated residual sum of squares between Model 1 and Model 2 indicate that Model 1 provided overall better simulation than Model 2 (Fig. 1). In the growing season (i.e., Apr. through Sep.; Fig. 1), Model 2 substantially over-estimated the soil temperature in the organic layers by approximately 5 °C at the dry site 1921D. For all sites at 30-cm depth, the soil temperatures simulated by Model 2 were over 2° warmer than the measured values for about half the growing season across all sites and by 1–2° for another 25% of the growing season. The inclusion of heat transport by water in Model 1 significantly improved the simulation of soil temperature during the growing season over Model 2 and reduced the discrepancies between measured and simulated values to be less than 1 °C. The still large discrepancies at 30 cm and 43 cm depths for 1964W and at 30 cm and 43 cm depths for the winter of 1930D might be caused by the inaccurately interpolated soil moisture, uncertainties associated with the estimates of the unsaturated water movement, and/or absence of heat produced by the biotic decomposition of OC in the winter (Khvorostyanov et al., 2008).

Comparisons of daily heat flux (DHF) during the growing season indicated that conduction contributed approximately 93%, 93%, 39%, and 56% of surface DHF (at 6 cm depths), and 20–28%, 50–67%, 32–42%, and 96–100% of deep DHF (i.e., at 30 cm and 43 cm depths) for 1964D, 1930D, 1921D, and 1964W, respectively. Liquid water movement contributed 7%, <1%, 61%, and 44% of DHF at 6 cm depth, and 72–80%, 33–50%, 58–68%, and 0–4% of DHF at 30 cm and 43 cm depth during the growing season. Vapor movement contributed ~7% of surface DHF (during the growing season at 6 cm depth) for 1930D, which has significantly lower moisture content than the other three sites, while vapor contributed less than 0.1% of DHF for other soil depths and sites during both winter and growing seasons. These results indicated that the impact of water movement on DHF was significant during the growing season in drier boreal sites whereas conduction dominated heat transport through the wet site.

Model 1 and Model 2 provided similar simulations for soil temperatures during the winter season (i.e., Oct. through Mar.; Fig. 1). The calculated DHF of each component of heat transport (i.e., conduction, liquid water, and water vapor) indicated that pure conduction contributed 89–100%, 89–100%, 92–94%, and 96–100% of DHF during the winter season for 1964D, 1930D, 1921D, and 1964W, respectively, suggesting that heat was transported mainly by conduction when the soil is frozen due to the limited liquid water content.

To illustrate the importance of representing water movement in the heat transport model, we evaluated soil thermal dynamics (and potential permafrost degradation) under the context of warming climate. Two warming scenarios projected by 1) the National Center for Atmospheric Research Parallel Climate Model (NCAR PCM A2) and 2) the Center for Climate System Research/National Institute for Environmental Studies (CCSR/NIES A2) (data obtained from http://www.ipcc-data.org) were simulated for the next 90 years (2010–2100). Several recent studies (Prunty and Bell, 2005; Zeller and Nikolov, 2000) indicated that the simulated soil temperatures using soil thermal models were strongly sensitive to the depth of lower boundary condition. Unless the measured soil temperatures are available to be used as the lower boundary condition, the depth of lower boundary should be deep enough (>10 m) to reasonably simulate the propagations of seasonal, annual, and decadal temperature signals during the long-term simulations (e.g., 100 years) (Prunty and Bell, 2005; Zeller and Nikolov, 2000). In our study, the lower boundary of simulated soil column was set to 20 m. The layer thickness at the top was 0.01 m and then increased for each layer by a factor of 1.05, resulting in thickness of 0.93 m at the bottom of soil column. The soil moisture content below 1.0 m soil depth was assumed to be at 100% saturation with no water movement based on the field observations. As a result, the energy flux below 1.0 m soil depth was exclusively controlled by heat conduction. Below the depth of 1.0 m, the initial soil temperature increased by a factor of 0.03 °C/m. The model was first spun up to reach an equilibrium state where the

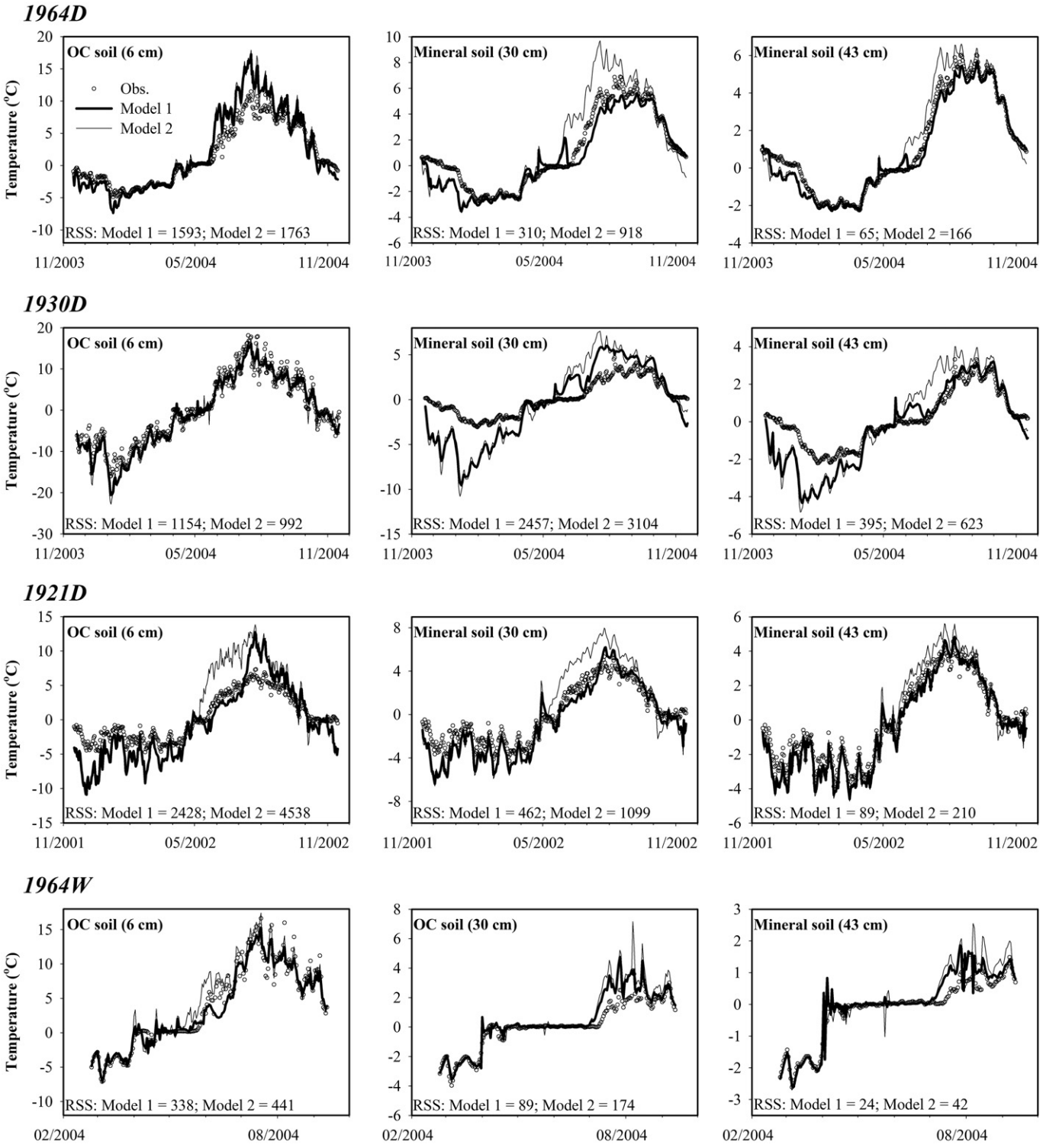


**Fig. 1.** Measured and simulated soil temperatures at three different soil depths (6, 30, and 43 cm) for the four black spruce forest sites (1964D, 1930D, 1921D, and 1964W). "Model 1" refers to the model where heat was transported by conduction, movement of liquid water, and movement of water vapor. "Model 2" refers to the model where heat was transported exclusively by conduction.

soil temperature differences between two consecutive time steps were less than 0.0001 °C through the soil profile. Other soil physical properties (e.g., organic layer thickness, soil moisture pattern, and soil thermal conductivities) were assumed to remain unchanged during the simulation. The upper boundary condition was set to the measured soil surface temperature at 0-cm depth plus the designed temperature increase (A2 scenarios from the NCAR PCM and CCSR/NIES). A time-dependent heat flux condition was assumed to be the lower boundary condition for the energy equation. The heat flux was calculated based on the following equation,

$$J = -K_t \frac{\partial T}{\partial z} \tag{12}$$

where $J$ is the heat flux density (J $cm^{-2} day^{-1}$).

Both Model 1 and Model 2 indicate that soil temperatures at a given soil depth linearly increased with the warming climate regardless of soil drainage condition. However results of Model 1 are strikingly different from Model 2 and indicate that the soil temperature increase at 30 cm and 90 cm depths was related to distribution of soil moisture content and physical properties of each site (Fig. 2). Soil drainage class has been identified in prior work as a key control on energy transport and a key factor in boreal soil responses to climate change (Yi et al., 2007). In prior modeling work however, wet sites with deep OC layers tend to warm more slowly than dry sites with shallow OC layers, an observation that has been attributed to the slower conductive heat transport through deeper OC layers (relative to shallow soils). Evaluated in the context of future changes in climate, such modeling analyses suggest that drier sites with shallow soil organic matter layers would be most vulnerable to warming and associated changes in soil processes (Yi et al., 2007) whereas the wetter site would be more resistant to permafrost degradation. In contrast, this study suggests that it is actually the wet sites with deep OC layers that would experience larger proportional increases in soil temperature with a given warming scenario when compared to the drier sites.

The more accurate simulations of Model 2 provide one line of support for our suggestion that wetter sites may be more vulnerable to permafrost degradation under a warming climate. A more substantial level of support for these conclusions is the recent field observation of permafrost degradation in Canada. Against a backdrop of rapidly warming temperatures over the past three decades, Veldhuis et al. (2002) report that 67% of the poorly drained sites (12 out of 18 sites) and only 13% of the well drained sites (2 out of 15 sites) underwent significant changes (loss or degradation) in near surface permafrost (within 120-cm depth) during the last 30 years (1970–2000) in North-Central Manitoba, Canada. These recent field-based studies combined with the simulations of future warming strongly suggest that permafrost under thick OC layers will be more vulnerable to warming than permafrost under well drained sites with thin OC layers.

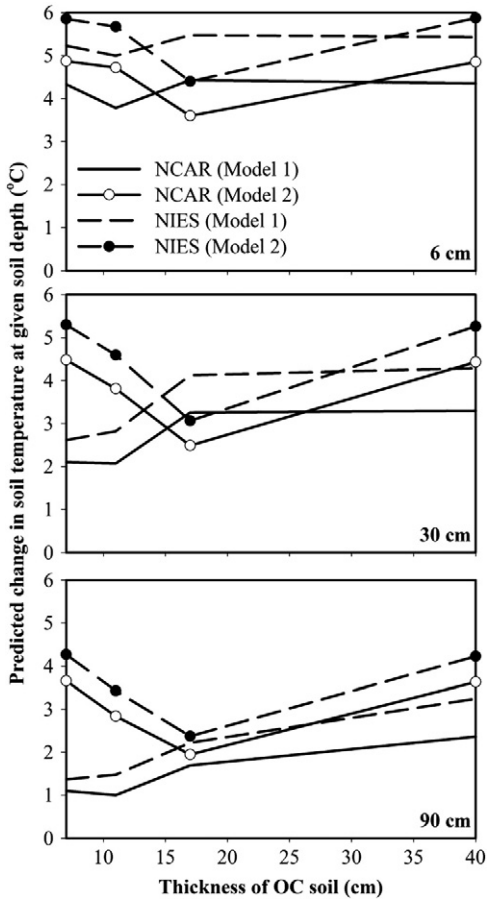


**Fig. 2.** Changes in soil temperature in wet and dry sites at the end of the simulation of two warming scenarios (NIES/CCSR A2 and NCAR PCM A2) using Models 1 and 2.

The mechanisms that underlie these differences in soil response to temperature change are complex and involve the combined influence of conduction and water-related heat transport (and variable contributions of these two factors across sites). The over-estimation of soil temperatures in the dry site by conduction-only models and the differential response of these sites to warming appear to be related to the transport of water through soils. The upward gradients of water potential energy (mainly due to the upward moisture gradient) 1) in the mineral soils of dry sites and 2) in the humic OC and mineral soils of wet sites cause significant upward liquid water movement. Since the temperature of the deeper soil layers is lower than that of the shallow soil layers, the upward water movement lowers the temperature of upper soil layers, which also explains why soil temperatures simulated by the convection Model 1 in summer are lower than by the conduction-only Model 2. Such upward water movement is well documented in mineral soils (e.g., Dingman, 1993; Hansson et al., 2004; Richards, 1941) and has been reported for sphagnum moss dominated peatlands and wetlands (e.g., Devito et al., 1998; Reeve et al., 2000; Romanowicz et al., 1993). The net effect of this heat transport via water movement is the cooling of surface layers and appears to be an important contributor to the mismatch between Model 2 simulations and observed temperatures.

Soil depth and moisture content also play an important role in the propagation of warming climate through soils. In general, deeper soil layers experience less increase in soil temperature. Thus atmospheric warming leads to large vertical gradients in soil temperature. Because heat transport in the wet sites is dominated by conduction (96–100% of deep DHF as discussed earlier) due to the limited water movement and low hydraulic conductivity, warming causes more increase in deep soil temperature in the wet sites than in the dry sites. In drier sites, the upward convection of heat in liquid water that results in the cooling of surface layers also appears to reduce the vulnerability of these sites to warming by reducing the energy flux to deeper soil layers.

## 4. Conclusions

Permafrost in the boreal region has been warming as a result of climate warming during the last several decades (Jorgenson et al., 2001; Lemke et al., 2007; Yoshikawa et al., 2003). This study indicates that water movement through boreal soil is a critical factor for accurate simulations of energy (heat) transport into boreal ecosystems and changes both the quantitative and qualitative predictions of landscape scale permafrost degradation. These findings, if accurate, have wide implications for projections of boreal response to climate. A large fraction (approximately 33–37%) of terrestrial C is stored in northern soils and poorly drained sites contain the vast majority of the C stores in the upper 3 m of northern ecosystems (Tarnocai et al., 2009a). If these sites also are the most vulnerable to warming-induced permafrost loss as suggested here, then there would also be a higher potential for destabilization of these large C reserves and release of additional $CO_2$ and $CH_4$ from these ecosystems over the coming decades.

## Acknowledgements

This modeling research was supported by the National Institute for Climate Change Research, U.S. Department of Energy (DOE-NICCR; grant #: MPC 35UT-01) and the US National Aeronautics and Space Administration (NASA; grant #: NNX06AE65G). Field research was supported by the U.S. National Science Foundation, the U.S. Department of Energy, the U.S. Geological Survey, and the Natural Resources Canada programs. We thank C.S. Carbone, M. Goulden, S.

Trumbore (University of California at Irvine), K. Manies, and L. Pruett (U.S. Geological Survey) for their assistance in the field and/or laboratory experiments. Also, we greatly appreciate the helpful comments from A.D. McGuire (USGS/University of Alaska at Fairbanks (UAF)) and F. Yuan (UAF).

## Appendix A. Supplementary data

Supplementary data to this article can be found online at doi:10.1016/j.scitotenv.2011.02.009.

## References

Agafonov L, Struck H, Nuber T. Thermokarst dynamics in Western Siberia: insights from dendrochronological research. Palaeogeogr Palaeoclimatol 2004;209:1–4.
Bond-Lamberty BP, Wang C, Gower ST. Net primary production and net ecosystem production of a boreal black spruce wildfire chronosequence. Glob Change Biol 2004;10:473–87.
Cahill AT, Parlange MB. On water vapor transport in field soils. Water Resour Res 1998;34:731–9.
Committee CASC. The Canadian system of soil classification. Ontario, Canada: National Research Council Canada Research Press; 1998.
Devito KJ, Waddington JM, Branfireun BA. Flow reversals in peatlands influenced by local groundwater systems. Hydrol Process 1998;11:103–10.
Dingman SL. Physical hydrology. Englewood Cliffs, NJ: Prentice Hall; 1993.
Fan Z, Neff JC, Harden JW, Wickland KP. Boreal soil carbon dynamics under a changing climate: a model inversion approach. J Geophys Res 2008:113 G04016.
Germann PF. Kinematic wave approach to infiltration and drainage into and from soil macropores. Trans Am Soc Agric Eng 1985;28:745–9.
Hansson K, Simunek J, Mizoguchi M, Lundin L, Van Genuchten MT. Water flow and heat transport in frozen soil: numerical solution and freeze–thaw applications. Vadose Zone J 2004;3:693–704.
Harden JW, Maines KL, Turetsky MR, Neff JC. Effects of wildfire and permafrost on soil organic matter and soil climate in interior Alaska. Glob Change Biol 2006;12: 2391–403.
Jones PD, Moberg A. Hemispheric and large-scale surface air temperature variations: an extensive revision and an update to 2001. J Climate 2003;16:206–23.
Jorgenson MT, Osterkamp TE. Response of boreal ecosystems to varying modes of permafrost degradation. Can J For Res 2005;35:2100–11.
Jorgenson MT, Racine CH, Walters JC, Osterkamp TE. Permafrost degradation and ecological changes associated with a warming climate in central Alaska. Clim Change 2001;48:551–79.
Jury WA, Horton R. Soil physics. Hoboken, New Jersey: John Wiley & Sons, Inc; 2004.
Kane DL, Hinkel KM, Goering DJ, Hinzman L, Outcalt SI. Non-conductive heat transfer associated with frozen soils. Glob Planet Change 2001;29:275–92.
Khvorostyanov DV, Krinner G, Ciais P, Heimann M, Zimov SA. Vulnerability of permafrost carbon to global warming. Part 1: model description and role of heat generated by organic matter decomposition. Tellus Ser B 2008;60:250–64.
Lemke P, Ren J, Alley RB, Allison I, Carrasco J, Flato G, et al. Observations: change in snow, ice and frozen ground. In: Solomon S, Qin D, Manning M, Chen Z, Marquis M, Averyt KB, et al, editors. Climate change 2007: the physical science basis, contribution of working group I to the fourth assessment report of the intergovernmental panel on climate change. United Kingdom and New York, USA: Cambridge University Press; 2007.
Litvak M, Miller S, Wofsy SC. Effect of stand age on whole ecosystem $CO_2$ exchange in Canadian boreal forest. J Geophys Res 2003;108.
Lu S, Ren T, Gong Y, Horton R. An improved model for predicting soil thermal conductivity from water content at room temperature. Soil Sci Soc Am J 2007;71: 8-14.
Lundin L. Simulated physical effects of shallow soil heat extraction. Cold Reg Sci Technol 1985;11:45–61.
Manies KL, Harden JW, Veldhuis H. Soil data from a moderately well and somewhat poorly drained fire chronosequence near Thompson, Manitoba, Canada. U.S. Geological Survey Open File Report 2004–1271; 2006. p. 19.
Manies KL, Harden JW, Yoshikawa K, Randerson J. The effect of soil drainage on fire and carbon cycling in central Alaska. U.S. Geol. Surv. Prof. Pap. 1678. Reston, Va: U.S. Geol. Surv; 2003.
Mdaghri-Alaoui A, Germann PF. Kinematic wave approach to flow and moisture during infiltration and redistribution of water in a structured soil. Hydrol Sci J 1998;43: 561–78.
O'Donnell JA, Romanovsky VE, Harden JW, McGuire AD. The effect of moisture content on the thermal conductivity of moss and organic soil horizons from black spruce ecosystems in Interior Alaska. Soil Sci 2009;174:646–51.
Ping CL, Michaelson GJ, Jorgenson MT, Kimble JM, Epstein H, Romanovsky V, et al. High stocks of soil organic carbon in the North American Arctic region. Nat Geosci 2008;1:615–9.
Price JS, Whittington PN, Elrick DE, Strack M, Brunet N, Faux E. A method to determine unsaturated hydraulic conductivity in living and undecomposed *Sphagnum* moss. Soil Sci Soc Am J 2008;72:487–91.
Prunty L, Bell J. Soil temperature change over time during infiltration. Soil Sci Soc Am J 2005;69:766–75.
Rapalee G, Trumbore SE, Davidson EA, Harden JW, Veldhuis H. Soil carbon stocks and their rates of accumulation and loss in a boreal forest landscape. Glob Biogeochem Cycles 1998;12:687–701.
Reeve AS, Siegel DI, Glaser PH. Simulating vertical flow in large peatlands. J Hydrol 2000;227:207–17.
Richards LA. Hydraulics of water in unsaturated soils. Agric Eng 1941;22.
Romanowicz EA, Siegel DI, Glaser PH. Hydraulic reversals and episodic methane emissions during drought cycles in mires. Geology 1993;21:231–4.
Saito H, Simunek J, Mohanty BP. Numerical analysis of coupled water, vapor, and heat transport in the vadose zone. Vadose Zone J 2006;5:784–800.
Schaap MG, Leij FJ, Van Genuchten MT. ROSETTA: a computer program for estimating soil hydraulic properties with hierarchical pedotransfer functions. J Hydrol 2001;251:163–76.
Simunek J, Jarvis NJ, van Genuchten MT, Gardenas A. Nonequilibrium and preferential flow and transport in the vadose zone: review and case study. J Hydrol 2003;272: 14–35.
Singh P, Spitzbart G, Hubl H, Weinmeister W. Hydrological response of snowpack under rain-on-snow events: a field study. J Hydrol 1997;202:1–4.
Smith LC, Sheng Y, MacDonald GM, Hinzman LD. Disappearing arctic lakes. Science 2005;308:1429.
Smith TM, Reynolds RW. A global merged land–air–sea surface temperature reconstruction based on historical observations (1880–1997). J Climate 2005;18: 2021–36.
Soil Survey Division Staff. Soil Survey Manual. USDA HandbookWashington, DC: USDA; 1993.
Soil Survey Division Staff. Keys to soil taxonomy. Washington D.C., USA: National Resources Conservation Service, U.S. Department of Agriculture; 1998.
Striegl RG, Dornblaser MM, Wickland KP, Raymond PA. Carbon export and cycling by the Yukon, Tenana, and porcupine rivers, Alaska, 2001–2005. Water Resour Res 2007;43:W02411.
Tarnocai C, Canadell JG, Schuur EAG, Kuhry P, Mazhitova G, Zimov S. Soil organic carbon pools in the northern circumpolar permafrost region. Glob Biogeochem Cycles 2009a;23:GB2023.
Tarnocai C, GCanadell JG, Schuur EAG, Kuhry P, Mazhitova G, Zimov S. Soil organic carbon pools in the northern circumpolar permafrost region. Glob Biogeochem Cycles 2009b;23:GB2023.
Veldhuis H, Eilers RG, Mills GF. Permafrost distribution and soil climate in the Glacial Lake Agassiz basin in North-central Manitoba, Canada. 17th World Conference on Soil Science, Bangkok, Thailand; 2002.
Verseghy DL. CLASS—a Canadian land surface scheme for GCMs, I, Soil model. Int J Climatol 1991;11:111–3.
Vitt DH, Halsey LA, Bauer IE, Campbell C. Spatial and temporal trends in carbon storage of peatlands of continental western Canada through the Holocene. Can J Earth Sci 2000;37:683–93.
Walvoord MA, Striegl RG. Increased groundwater to stream discharge from permafrost thawing in the Yukon River basin: potential impacts on lateral export of carbon and nitrogen. Geophys Res Lett 2007;34:L12402.
Wang C, Bond-Lamberty BP, Gower ST. Carbon distribution of a well- and poorly-drained black spruce fire chronosequence. Glob Change Biol 2003;9:1066–79.
Weiss R, Shurpali NJ, Sallantaus T, Laiho R, Laine J, Alm J. Simulation of water table level and peat temperatures in boreal peatlands. Ecol Model 2006;192:441–56.
Wolf A, Callaghan TV, Larson K. Future change in vegetation and ecosystem function of the barents Region. Clim Change 2008;87:51–73.
Yi S, Woo MK, Arain MA. Impacts of peat and vegetation on permafrost degradation under climate warming. Geophys Res Lett 2007;34:L16504.
Yoshikawa K, Bolton WR, Romanovsky V, Fukuda M, Hinzman L. Impacts of wildfire on the permafrost in the boreal forests of Interior Alaska. J Geophys Res 2003;108: 8148.
Zeller KF, Nikolov NT. Quantifying simultaneous fluxes of ozone, carbon dioxide and water vapor above a subalpine forest ecosystem. Environ Pollut 2000;107:1-20.
Zhang Y, Li C, Trettin CC, Li H, Sun G. An integrated model of soil, hydrology, and vegetation for carbon dynamics in wetland ecosystems. Glob Biogeochem Cycles 2002;16:1-17.